

Using machine learning to segment and quantify the neuropil space in the brain of the North American beaver (*Castor canadensis*)

Juliana Bourne¹, David Cain¹, Kathleen Bitterman¹ and Muhammad A. Spocter^{1,2,3}

¹Department of Anatomy, Des Moines University, Des Moines; ²School of Anatomical Sciences, Faculty of Health Sciences, University of the Witwatersrand, Republic of South Africa; ³Department of Biomedical Sciences, Iowa State University Vet Med.

Abstract

The North American beaver (*Castor canadensis*) is a large rodent species native to North America. Like most rodents, beavers have smooth (lissencephalic) brains however, this external organizational simplicity is contradicted by their apparent behavioral complexity (e.g., dam building), raising the question as to how beavers can perform these complex tasks with such diminutive brain organization. To address this question and develop an approach which could be readily applied to other understudied species, we surveyed the neuropil space (a proxy for cortical connectivity) using a combination of design based stereological sampling and machine learning. A sub sample consisting of image stacks of the frontal and visual cortex of the beaver brain were manually labelled and four models were developed and trained using varying sampling parameters. The resulting output from each model was then visually compared for accuracy to select the most optimal model for use. The results of this pilot study are discussed in consideration of the feasibility, accuracy, and challenges to ongoing analysis of the beaver cortical surface.

Introduction

The North American beaver is our largest rodent species (body mass 25 kg, body length 600-800 mm). Beavers are semi-aquatic and are found primarily along lakes and streams where they build complex dams, lodges and canals. Given their reliance and proximity to these natural water sources, beavers are considered an important keystone species for monitoring the health of our wetlands. They are nocturnal and during the winter months will spend much of their time in their lodge, leaving only to collect food from their food cache.



Figure 1: A photograph of the North American beaver (National Geographic.com)

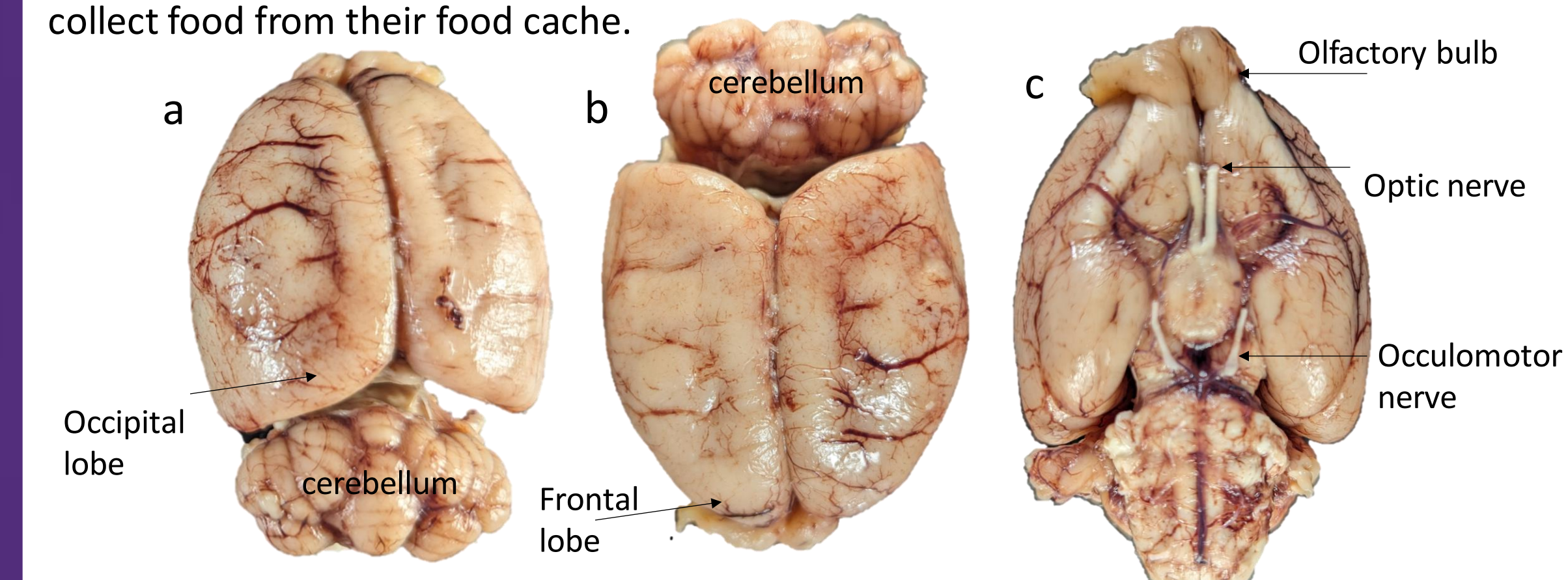


Figure 2: Photographs of the beaver brain. a- Caudal view showing the cerebellum and posterior cortical surface; b- Superior view of the cortical and cerebellar surface; c- inferior view of the cortex, midbrain and cranial nerves.

The study sample consisted of the brain of one American beaver (*Castor canadensis*). The brain specimen was acquired as a donation to M.A.S. from Taxidermy of Iowa and regulated by the Iowa DNR. The specimen died without any known neurological complications. Whole-brain specimen was harvested postmortem with the approval of the Des Moines University Animal Care and Use Committee. The brain was removed at necropsy and immersed in 10% formalin within 14 hours of the subject's death. The brain was prepared for histology as previously described (Spocter et al., 2018). Each hemisphere was blocked with a coronal cut at the level of the precentral gyrus and another cut at the level of the angular gyrus. These slabs were cryoprotected by immersion in buffered sucrose solutions up to 30%, embedded in Tissue-Tek medium, frozen in a slurry of dry ice and isopentane, and sectioned at 40 μ m with a sliding microtome in the coronal plane. Every 10th section (400 μ m apart) was stained for Nissl substance with a solution of 0.5% cresyl violet to visualize the somal cytoarchitecture.

Methods

Image Acquisition

Image collection for Neuropil Fraction (NF) analysis was performed using a Nikon Eclipse 80i microscope equipped with a Ludl XY motorized stage Heidenhain z-axis encoder, and an Optronics MicroFire color videocamera coupled to a Dell PC workstation running Stereo- Investigator software. To measure the NF, first contours were drawn around the regions of interest under low power magnification (2 \times), then fractionator sampling was used (grid spacing of 1000 \times 1000 μ m) as implemented by the StereoInvestigator system to collect a series of 16 bit color image frames obtained in a systematic-random fashion with a 20 \times (0.5 N.A.).

Methods

Tissue sampling

Sampling was undertaken in the medial frontal lobe (i.e., cingulate cortex = ACC) and the lateral occipital lobe (i.e., primary visual cortex= V1). Identification of cortical was guided by the principal investigator with reference to murine and rodent cytoarchitectural atlases (Paxinos & Watson, 1997).

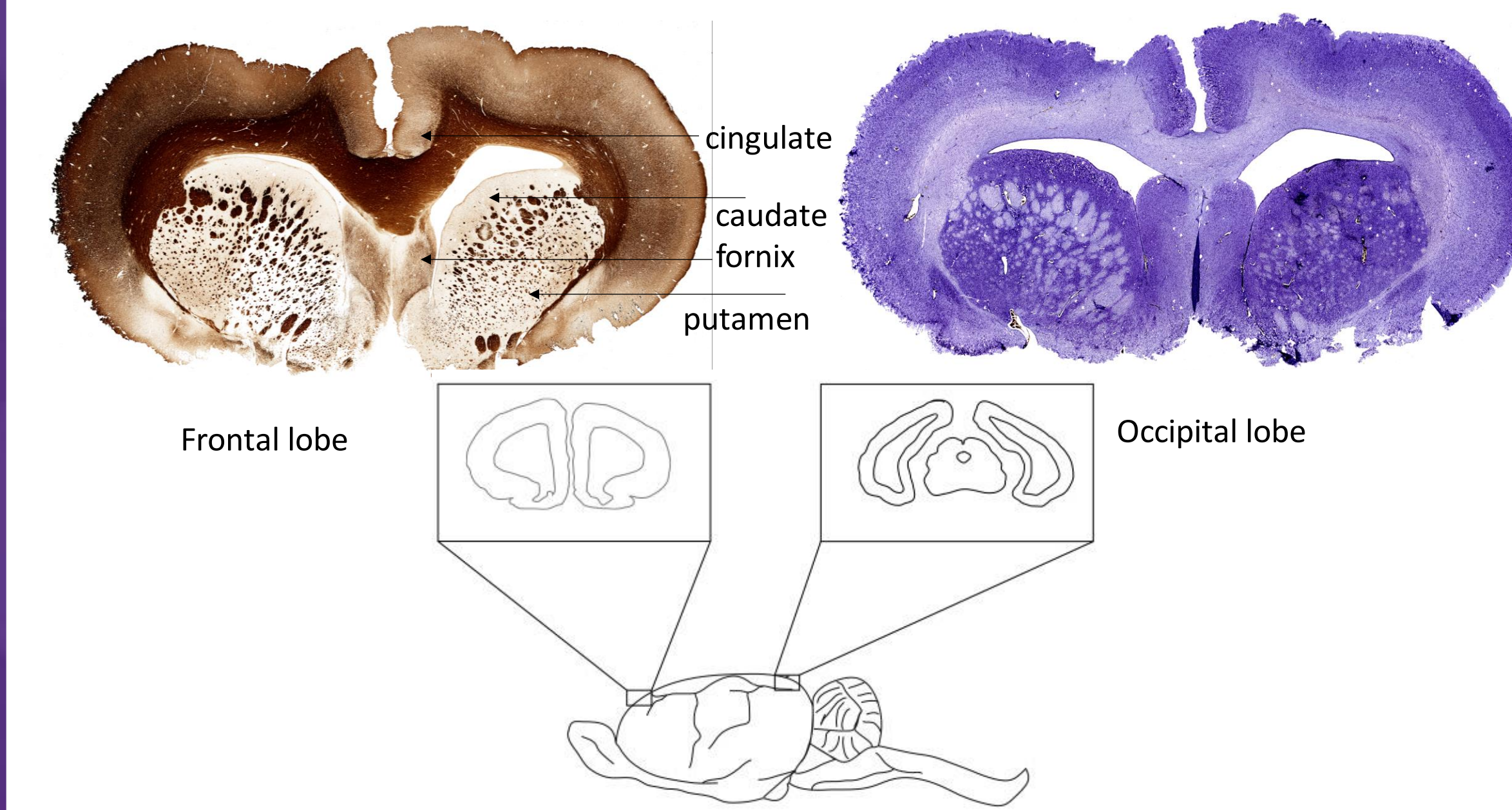


Figure 3: Schematic showing representative sampling of the ACC and V1 in the beaver brain along with coronal Nissl and Myelin sections through the frontal lobe showing the striatum.

Digital images from six Nissl-stained sections were analyzed for each region of interest. Throughout the process, image frame acquisition was monitored during fractionator sampling and all frames that fell outside of the boundaries of the region of interest were omitted from further processing. Image stacks consisting of ~20 images per section were collected. The following parameters describe the sampling design: grid spacing 1,000 μ m \times 1,000 μ m; image size 1,600 \times 1,200 pixels, resolution 0.37 pixels per μ m. The average target intensity was locked at 71% to ensure that the exposure was kept uniform while sampling.

Image analysis using machine learning

Once images were captured, each image series was imported into Orbit Image Analysis for automated segmentation of the neuropil space using machine learning (Stritt, Stalder, & Vezzali, 2020). Using the Model toolset in OrbitImage Analysis, we defined our classes of tissue (i.e., Foreground = cells; background = Neuropil). Once the classes were defined, we used the drawing tools under the Classification tab to manually label our classes of interest in a sample of images drawn from our dataset. To facilitate accurate training of the dataset, we made sure to outline regions that were close to the borders of each of our classes and also to sample across the images to ensure that the training dataset included a range of image intensity values.

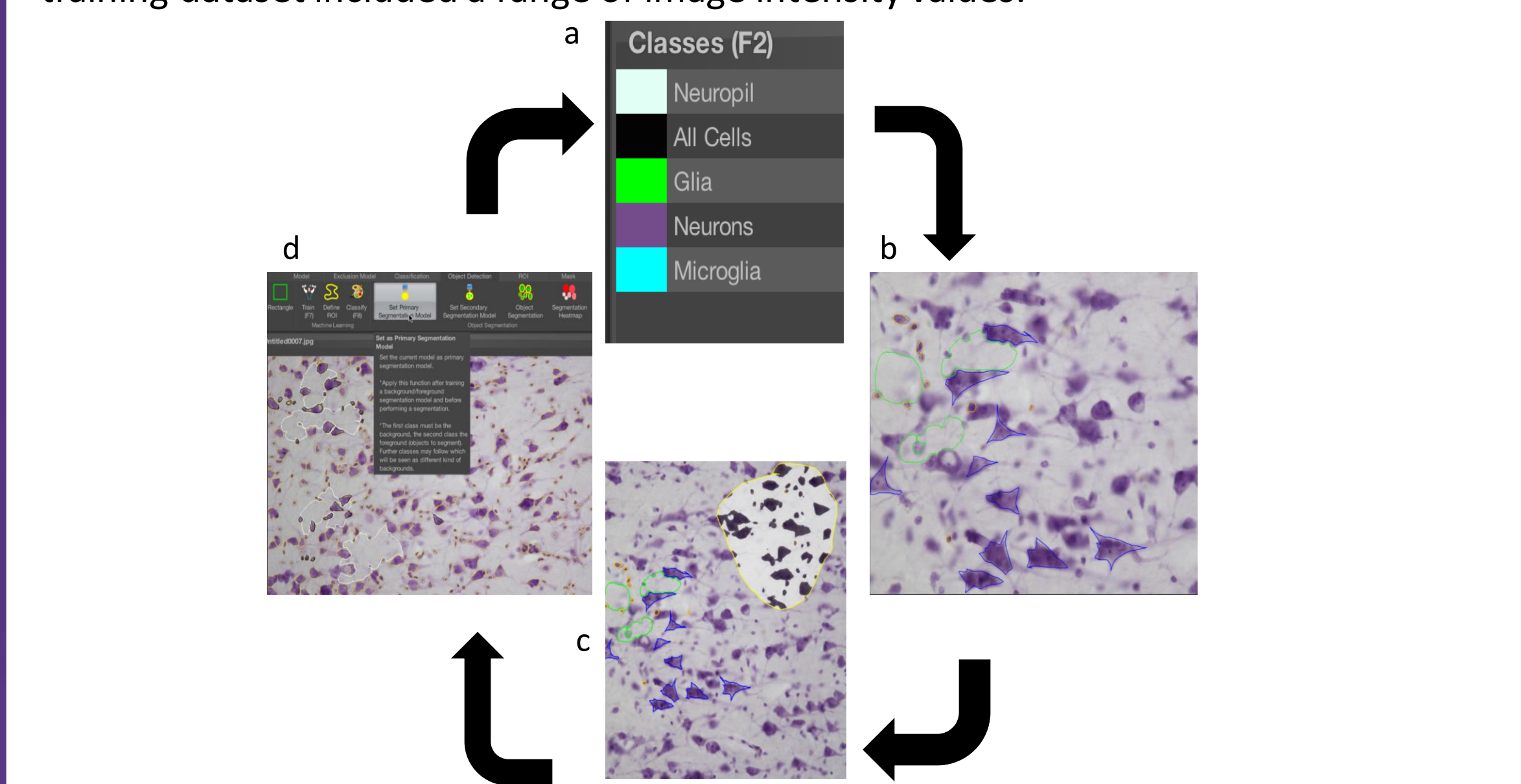


Figure 4: Workflow summary as screenshots from OrbitImage Analysis for the application of machine learning to a histology dataset. a- Define classes; b- Classify and Train dataset; c- ROI testing and accuracy inspections or Batch processing; d- Object segmentation for quantification of number of objects or size parameters

Methods

After the classification system was setup, the model was then built and trained.

Average model training took between 10-20 seconds depending on the number of images included in the image stack. After the model was trained, we used the Region of Interest (ROI) tool to define a region within our sample and visually inspected the results to evaluate the accuracy of the classification model. Models were then saved before being applied to the entire image dataset using the Batch processing function. An optional step within our analysis allowed us to quantify the number of objects in our segmented images. To perform these analyses were used the Object segmentation tools to define foreground and background components before loading the model with the predefined classes and labels to extract the number and size of segmented objects in our dataset. Data were compared across models to determine if more sampling sites in the initial training would change the accuracy of the model.

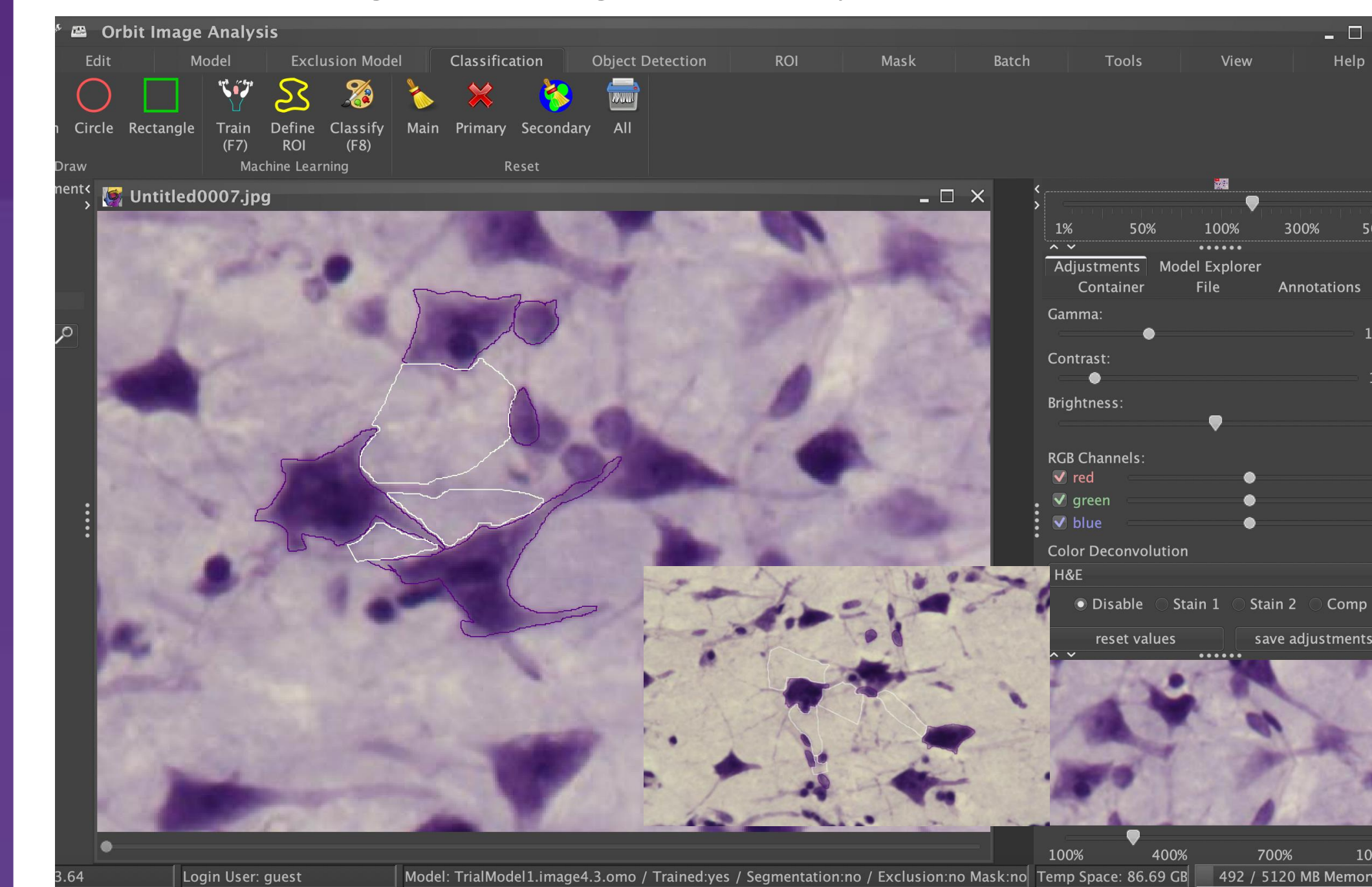


Figure 5: Screenshots showing examples of suitable classification and labelling necessary for model training of the neuropil space. Note that the investigator outlined adjacent areas on either side of select cells so that the model could learn the intensity differences associated with cellular profiles and distinguish this from the neuropil.

3D reconstructions from serial sections

In addition serial coronal sections of the beaver brain were imported into the 3D reconstruction program Reconstruct (Fiala, 2005) and used to make 3 dimensional volumes of the external surface of the beaver brain. In accordance with the procedures outlined with (Fiala, 2005) images were imported into the software, calibrated, aligned and then regions of interest were manually traced using the tracing tool function.

Results & Discussion

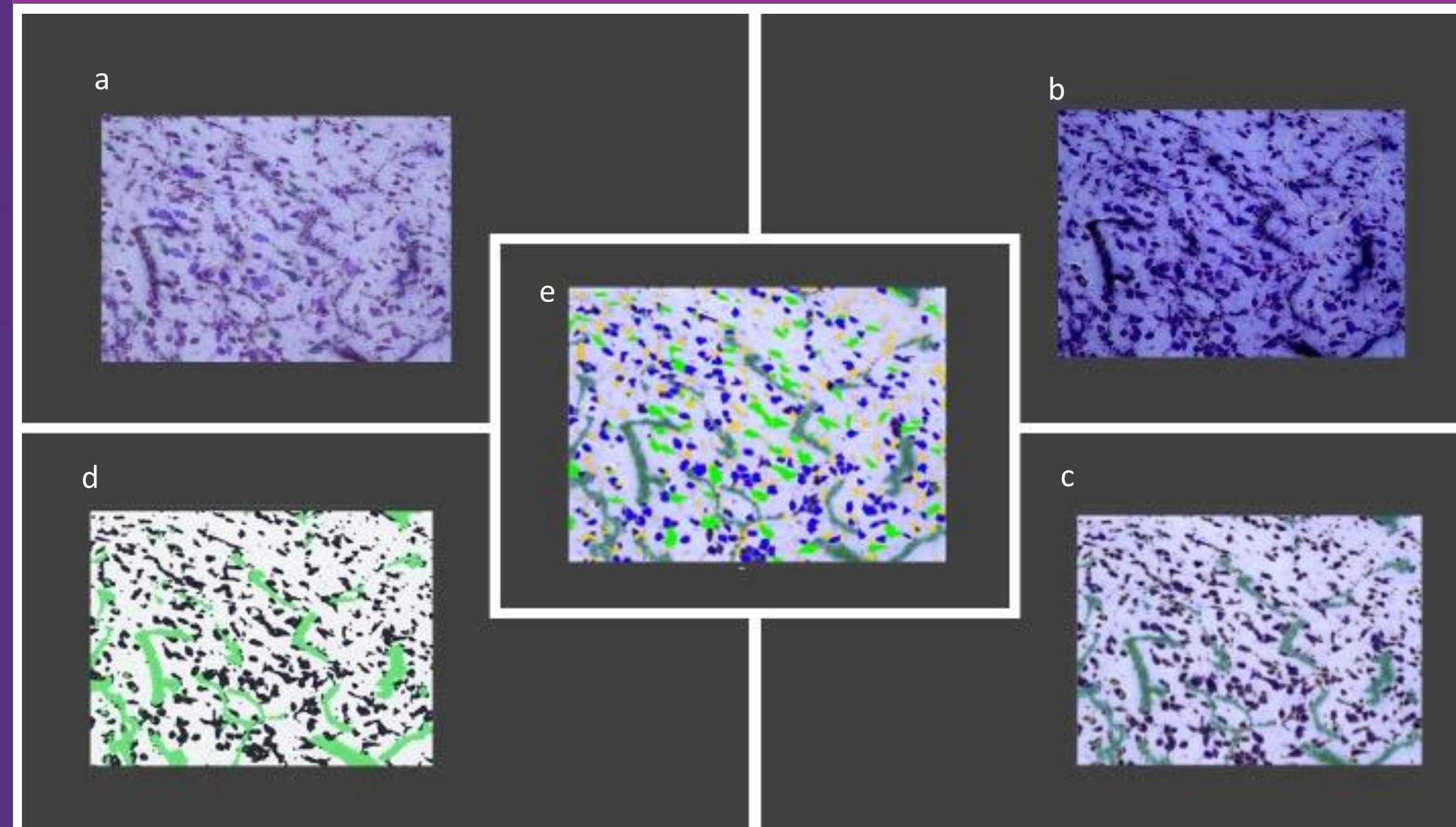


Figure 6: Screenshots showing examples of cellular and neuropil profiles segmented after machine learning. Note that in these examples, three classes were defined (Foreground= cells, background= neuropil; Vascular elements = capillaries). a = original image, b & c = opacity change 10-50%; d =100 opacity; e = full segmentation

Results & Discussion

Four models were trained with different ratios of neuropil and cell sampling sites: 3:5, 5:10, 7:15, 9:20, respectively. Samples included varying shades, shapes, and sizes of cells. All models were then used to batch process every slide in each section of the brain, saving considerable time. The models appeared to account for outliers, regardless of the amount of sampling sites initially used in training. Batch processing did not affect the accuracy of the models in this sample and streamlined tissue quantification. There was a bit of concern about the accuracy in certain sites with low intensity values (due to thicker sections) and the models incorrectly labelling cellular/neuropil profiles. In addition, the observer had to make a visual decision on the whether the models were "sufficiently trained" a factor which we felt added some subjectivity to the process. Based on our observations on the variance between models, we recommend that at a minimum approximately five images (See dimensions in Methods Section) should be used to sufficiently train the model to accurately quantify the neuropil space. The robustness of this recommendation is yet to be validated in another model species and using other datasets with more variable image quality. We also conclude that experimental scanning of histological image datasets to create 3D models of the brain space is feasible although not without challenges for visualization of the external surface.

Variation in the proportion of neuropil space (NF) & proportion of cells (All cells) estimated in 8 trials using different starting tissue sections and varying the number of labelled objects (i.e., number of Neuropil sites, number of Cell sites).

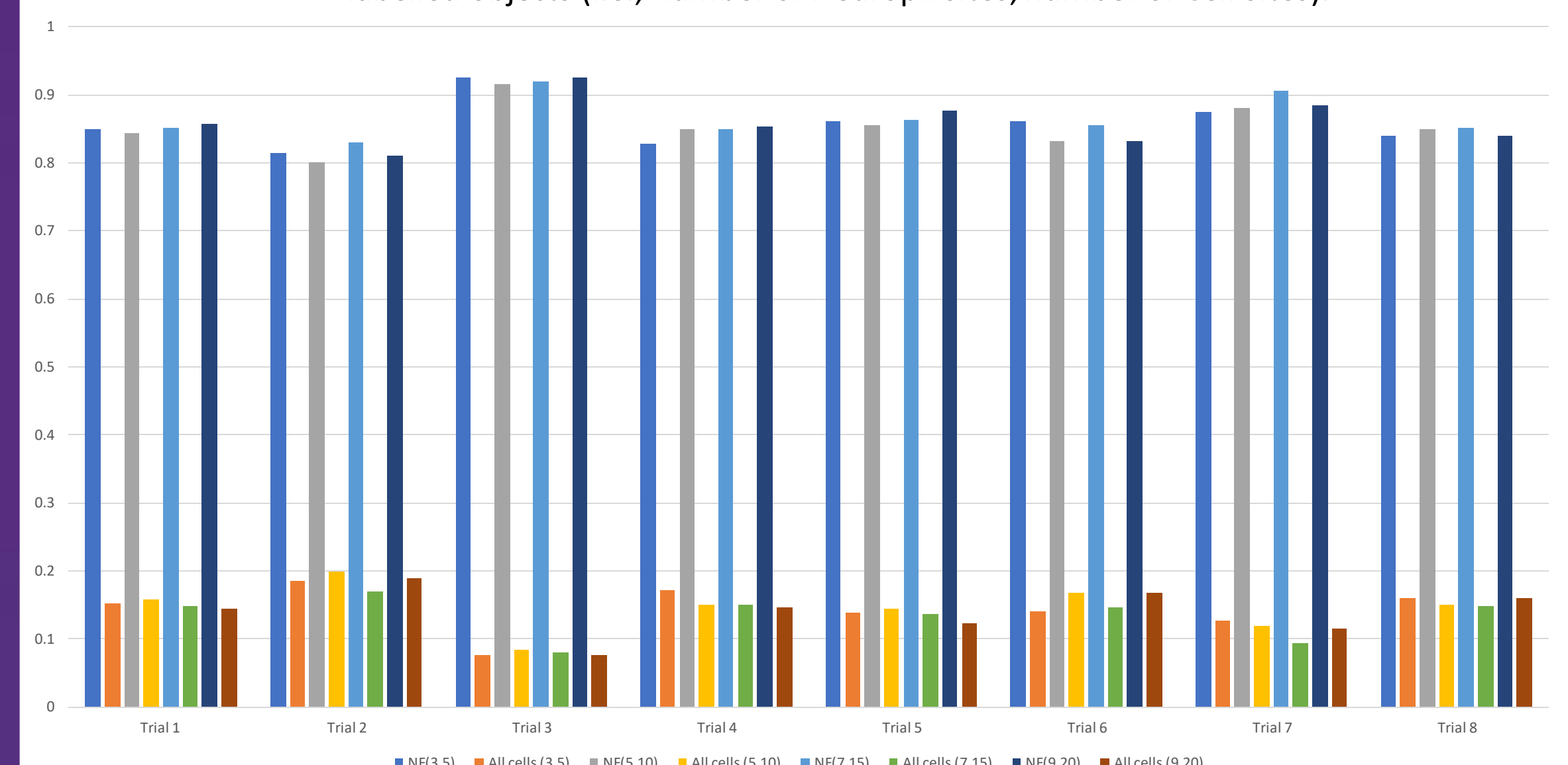


Figure 7: Variation in the proportion of neuropil space (NF) & proportion of cells (All cells) estimated in 8 trials using different starting tissue sections. Note that with each section the number of labelled objects (i.e., number of Neuropil sites, number of Cell sites) were varied. Note that the proportion of NF and All Cells varies between 0-1 in each case thus represents a percentage of space 0-100% occupied by neuropil or cells respectively.

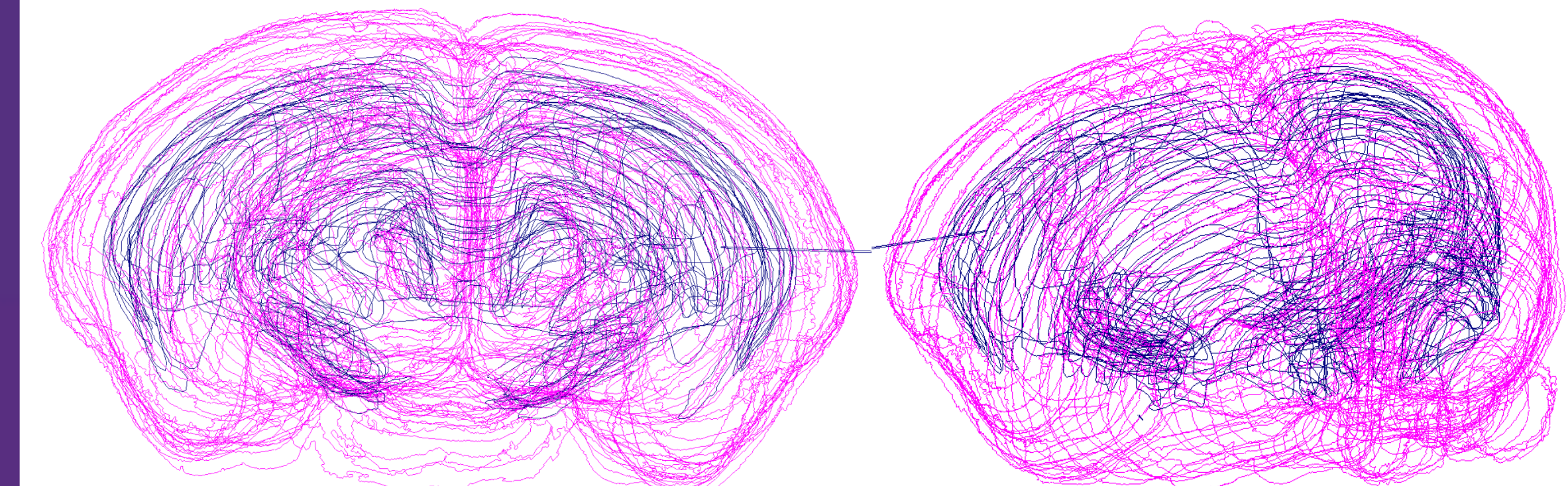


Figure 8: Screenshots showing the pilot reconstructions of scanned histological sections of the beaver brain (from Brainmuseum.org) segmented and reconstructed in 3D.

References

Spocter, M.A., Fairbanks, J., Locey, L., Nguyen, A., Bitterman, K., Dunn, R., Sherwood, C.C., Geletta, S., Dell, L.A., Patzke, N & Manger, P.R (2018). Neuropil distribution in the anterior cingulate and occipital cortex of artiodactyls. *Anatomical Record (Hoboken)*, 301:1871–1881

Stritt M, Stalder AK, Vezzali E (2020) Orbit Image Analysis: An open-source whole slide image analysis tool. *PLoS Computational Biology* 16(2): e1007313.

Acknowledgments

This work was supported by funding from the Iowa STEM BEST (MAS). We are also grateful for our community partnership with the Des Moines School District (Central Campus) which has helped to foster interest in STEM fields through supporting high school student involvement in our research.